Determination of a Hydrofoil for the Propulsion System of the 2000 University of California, San Diego Human-Powered Submarine

Scott Ketcham, University of California, San Diego
Sarah Bupp, University of California, San Diego
Alexander Garcia, University of California, San Diego
Mike Scott, University of California, San Diego

9500 Gilman Drive
La Jolla, California 92093
scott_ketcham@juno.com

Abstract-UCSD students are building a Human Powered Submarine to compete against other schools and attempt to break the International Human Powered Vehicle Association (IHPVA) and World Record in July 2000. This year's submarine team has built a propulsion mechanism to drive a single oscillating horizontal foil through the water, very similar to how a mammal swims, to complete in the non-propeller division. In this experiment, a water tunnel was used to compare the lift to drag ratios of a straight and swept-back NACA 0012 symmetric foil with and without winglets.

Although data taken only at two different water velocities is not completely conclusive, it was determined that a swept back wing with winglets is the configuration that provides the highest lift to drag ratio of 97.9 ± 0.2 at an angle of attack of about 7 degrees. The swept wing without winglets showed the maximum lift to drag ratio of 170. It is clear from relative values of the other wing configurations and other know data of the NACA 0012 that this ratio is abnormally high and is disregarded. Winglets decreased the lift to drag ratio for the straight wing at both velocities. At the lower velocity of 1.4 m/s, the straight wing without winglets had a higher ratio compared to that of the swept wing with winglets. However, at a higher velocity, the swept wing with winglets had a higher ratio. Disregarding the abnormally high ratio of the swept wing with no winglets, it is determined that this configuration provides the highest lift to drag ratio. Thus, implementing a tail with a swept back wing with winglets will best propel the submarine to a very achievable IHPVA and World Record.

INTRODUCTION AND THEORY

I. Hydrofoil Theory

A NACA 0012 foil will be used in all of the wing configurations that will be tested in this experiment. This symmetric foil is known for its decent lift to drag ratio, good stall characteristics, and overall favorable flow characteristics. Minimizing tip area by using a high aspect ratio will reduce the intersection of the low pressure on the upper surface of the wing and the higher pressure on the lower surface of the wing. Where these different pressures meet at each wing tip, the higher pressure "spills" over onto the upper surface of lower pressure. This is commonly called "tip loss". Thus, an aspect ratio of six will be used for all wing configurations in this experiment.

The wing planform shape and the use of winglets to optimize the lift to drag ratio will be determined. A straight wing will first be tested at two different velocities. At each velocity, the wing will be taken through a twenty-degree range of angles of attack to compare the lift and drag forces. Winglets, small fins protruding approximately 90 degrees from the tip of the wing, will then be placed on the wing and will be tested at each velocity and angle of attack. Winglets can increase the lift to drag ratio of the wing, however, if the winglet is too large, its increase of drag would "out-weigh" the additional lift, and lower the overall lift to drag ratio.

0-933957-31-9

A swept back wing will then be tested at the same velocities and angles of attack. Sweeping back a wing can decrease its induced drag. According to research done by a biologist, Frank E. Fish in 1998, a tapered swept-back wing can achieve a higher efficiency by reducing induced drag by 8.8% compared to a wing with an elliptical planform area. Winglets will then be placed on this swept back wing and again studied at the same velocities and angles of attack. The results of the winglets on the swept back wing will be compared to all other wing configurations. The results of this study will determine further modifications, adjustments and tests to be made to a wing in order to determine the final wing specifications that will be used on the Human Powered Submarine.

II. Experimental Equipment Design

A sting force balance was designed in order to measure the lift and drag forces on each wing. The forces on the wing in the water tunnel may be resolved as shown below in Fig. 1.

Fig. 1. Forces on a Wing

By definition, lift is always perpendicular to flow and drag is always parallel to flow. Thus, forces in only these two directions must be measured. A schematic of the sting for this experiment is shown below in Fig. 2.

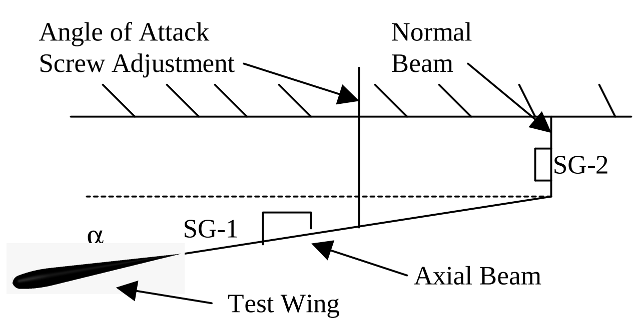

Fig. 2. Schematic of Sting Setup

This device will be used to hold the wing and measure the lift and drag forces while changing its angle of attack. Strain gauges (SG-1 and SG-2) are located on specific cantilevered beam members of the sting as shown above. These strain gauges are used to detect any deflection of the beams due to forces acting on the wing. These deflections cause a resistance change in the strain gauges, which will result in a voltage difference. This voltage difference will be read using Labview, and after calibration, will represent actual forces acting on the wing. SG-1 is the strain gauge that measures strain primarily due to lift and SG-2 is the strain gauge that measures strain primarily due to drag. The screw adjustment is used to change the angle of attack, which increases as the wing is lowered.

The size of the cantilever beams must be carefully planned in order to determine the appropriate strain gauges needed for the experiment. To do so, the maximum lift and drag forces on the NACA 0012 foil were calculated using the equations below:

$$L = 0.5\rho V^2 C_L A_p \tag{1}$$

$$D = 0.5\rho V^2 C_D A_p \tag{2}$$

Where ρ is the density of water, V is the maximum velocity of the water tunnel, C_L is the maximum coefficient of lift, C_D is the maximum coefficient of drag for a NACA 0012 foil, and A_p is the planform area of the wing.

The moment of inertia, slope, and deflection of each cantilever beam, as shown in Fig.3, were determined using the equations below. Finally, stress and strain were determined so that the proper strain gauges could be selected.

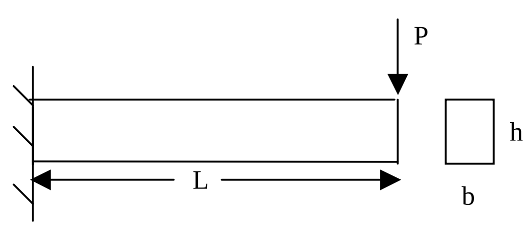

Fig. 3. Cantilever Beam with Basic Formulas

Moment of Inertia, $I = 1/12bh^3$ (3)

Slope at End of Beam, $\theta = PL^2/2EI$ (4)

Deflection at End of Beam, $\delta = PL^3/2EI$ (5)

Stress in Beam, $\sigma_{xy} = Pxy/I$ (6)

Strain in Beam, $\varepsilon = \sigma_{xy}/E$ (7)

PROCEDURE

I. a. Calibration of Angle of Attack

In order to properly analyze the strain gauge data gathered in this experiment, extensive calibration must be performed on the sting force balance. A means of determining the angle of attack must be implemented in this experiment for sting angles zero through twenty. This was done by measuring the angle of attack while counting the number of turns of the adjustment nut.

I. b. Sting Calibration

The voltages read from the strain gauges must be correlated to actual forces acting on the sting. Due to the unique design of the sting, the calibration method is complicated. Because of the geometry of the sting, the strain gauges on the axial beam are greatly affected by the forces acting on the normal beam. These interactions between the two beams must be calibrated. Because the sting is exposed to the flow of water, the force of the water acting on the sting must also be calibrated as a function of angle of attack and velocity. The overall drag and lift equations are determined by:

Drag Force = (Drag force read)-(axial force from normal beam)-(axial force from angle of attack)-(axial force from sting) (8)

Lift force = (Lift force read)-(Lift force from Drag)-(Lift force from sting) (9)

The voltage read from the strain gauges are calibrated by applying different forces on the axial and normal beams. A calibration curve is produced by correlating the voltage to the amount of force. A fit equation determines the force to voltage correlation to be:

Axial Beam: Force = 0.7489(Axial Voltage)+0.1196 (10)

Normal Beam: Force = -1.0257(Normal Voltage)+0.0021 (11)

The force transmitted to the axial beam from a pure lift force is calibrated by hanging weights from the sting in a horizontal position as seen in Fig. 4. Three different weights were used and then averaged to find a shape of the curve as a function of angle of attack. The magnitude of the force from the equation was determined to be

Axial Force = 0.047(Lift Force) (12)

The overall calibration of the amount of force acting on the axial beam from a pure normal force is a function of the magnitude of the force and angle of attack. The combination of these equations produces:

$$F_{Dn} = -0.00006(\alpha)^4+0.0025(\alpha)^3-0.0429(\alpha)^2+0.2413(\alpha)+0.047*F_L \quad (13)$$

where α is the angle of attack in degrees. Pure axial force also changes with angle of attack. To calibrate this, the sting was mounted in a vertical position and weight was hung to create a pure axial force as seen below in Fig. 4.

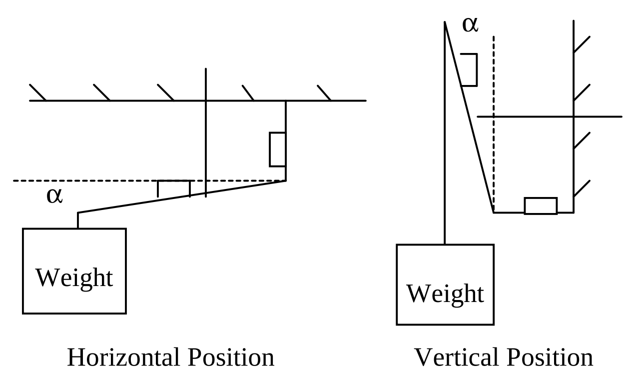

Fig. 4. Horizontal and Vertical Sting Calibration Positions

A fit equation for the amount that the pure axial force changed with angle of attack is determined to be:

$$\text{Axial Force} = -0.002(\alpha)^2+0.0094(\alpha) \quad (14)$$

The artificial lift force caused from pure drag is a function of angle of attack and amount of drag force. From simple geometry, the amount is determined to be:

$$F_{Ld} = (\text{Drag force})\sin(\alpha) \quad (15)$$

I. c. Calibration of Water Force on Sting

Because the sting feels the force of the water flowing around it during its operation, the sting must also be calibrated so that wing forces can be isolated. This will be done by placing the sting in the water tunnel without a test wing to determine the force that the water flow exerts on the sting as it travels through its range of angles of attack. The sting was placed in the water tunnel and the angle of attack was varied at two different water velocities. The data is averaged and the overall equation for the water force acting on the sting, as a function of the water velocity (V_w) and angle of attack (α), is determined to be:

$$\text{Axial force from water} =-0.0012(\alpha)^2-0.034(\alpha)+0.1692(V_w)^2+0.3863(V_w) \quad (16)$$

$$\text{Normal force from water} = -0.0086(\alpha)-0.3411(V_w)^2+0.2247(V_w) \quad (17)$$

Because drag force is a function of the lift force and the lift force is a function of the drag force, these two simultaneous equations must be solved. The total drag force is computed by plugging the lift force into the drag force equation and solving for the drag. The total drag equation is:

$$\text{Drag} = [0.7489(\text{axialvoltage})+0.1196+0.00006(\alpha)^4-0.0025(\alpha)^3+0.0429(\alpha)^2-0.2413(\alpha)-0.047((-1.0257(\text{normal voltage})+0.0021)/\cos(\alpha)+0.0086(\alpha)+0.3411(V_w)^2-0.2247(V_w))+0.002(\alpha)^2-0.0094(\alpha)+0.0012(\alpha)^2+0.0342(\alpha)-0.1692(V_w)-0.3863(V_w)]/(1-0.047*\sin(\alpha)/\cos(\alpha)) \quad (18)$$

where α is the angle of attack in degrees and V_w is the velocity of the water in meters per second. The total lift equation is then determined from:

$$\text{Lift} = [-1.0257(\text{normalvoltage})+0.0021-\text{Drag}*\sin(\alpha)]/\cos(\alpha)+0.0086(\alpha)+0.3411(V_w)-0.2247(V_w) \quad (19)$$

All the voltages from the experiment were read using the Sting.vi Labview program. A complete list of equipment used in the experiment is shown below in Table 1.

TABLE 1

Experimental Equipment List

Equipment Name	Model	Function
Impeller Motor Controller	Toshiba Tosvert 130H	Communicates desired frequency to impeller motor
Pressure Data Gathering Software	Scan Rotary Value.vi	Labview program which gathers data from Pitot-Static Tube
Strain Data Gathering Software	Sting.vi	Labview program which gathers voltages for each strain gauge
Strain Gauges	Micromeasurements Brand	Detects strain in cantilever beams

I. d. Calibration of Water Tunnel Using the Pitot-Static Tube

Next, the water tunnel speed must be calibrated. Frequencies of 15, 30, and 44 Hz are entered into the Toshiba

Tosvert 130H impeller motor controller. See the schematic of the water tunnel calibration equipment in Fig. 5 below.

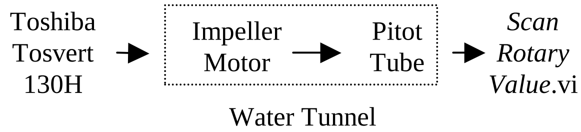

Fig. 5. Schematic of Water Tunnel Calibration Equipment

The motor speed adjusts accordingly and the water velocity in the tunnel changes. A time interval of two minutes is allowed before any data is taken to achieve steady state flow for proper water velocity measurements. Then a voltage proportional to the difference in static and freestream pressure is read with the Scan Rotary Valve.vi program. This voltage difference is linearly proportional to the pressure difference in water height.

$$\Delta h = 1.6325V + 0.0068 \tag{20}$$

where Δh is the pressure difference and V is the voltage read from the Scan Rotary Valve.vi program. Freestream velocity is calculated with the relation:

$$U_\infty = [(2\rho_p \Delta hg)/(\rho_f)]^{1/2} \tag{21}$$

where ρ_p is the density of water in the pitot tube, g is the earth's gravity, and ρ_f is the freestream density. In this experiment it is assumed that water is incompressible, so:

$$\rho_p = \rho_f. \tag{22}$$

Thus, the equation for freestream velocity simplifies to:

$$U_\infty = (2\Delta hg)^{1/2} \tag{23}$$

Now a plot of velocity vs. frequency can be generated from which an equation relating the two variables is obtained. This equation is a means for determining frequency for corresponding velocities.

II. Wing Testing

Now that the sting is properly calibrated, testing of the wing configurations may begin. Four different wing configurations are tested as seen in Table 2.

TABLE 2

Characteristics of Four Different Wing Configurations

Wing Configuration	**Straight Wing**	**Swept Back Wing**	**Winglets**
1	X		
2	X		X
3		X	
4		X	X

The straight wing without winglets is mounted to the sting and a frequency is entered into the Toshiba Tosvert 130H impeller motor controller in order to obtain a velocity of 1.4 m/s. Voltage values are gathered for the axial and normal strain gauges as the angle of attack is varied from zero to twenty degrees. A schematic of the experimental set-up is shown below in Fig 6.

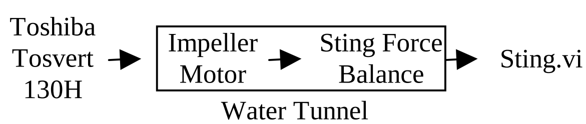

Fig. 6. Schematic of Experiment

The water velocity is then increased to 1.8 m/s and the voltage values of the axial and normal strain gauges are recorded as the angle of attack is varied again from zero to twenty degrees. The straight wing with winglets is then mounted to the sting and the data is recorded through the angles of attack at the two different water velocities.

The swept wing with and without winglets will now be analyzed. Special care must be taken to properly mount the center of pressure of each wing in the same location on the sting. It was determined that due to the 10 degree sweep angle of the swept wing, the wing was required to be mounted 0.24 inches forward to that of the straight

Once all the data is gathered, the lift and drag values are compared at each angle of attack. Equations are then fit to the curves to average the data for better comparison of the lift and drag of the different wing configurations. From the fit equations of each wing configuration, the lift to drag ratio is calculated and plotted to compare to one another. From these curves, the highest lift to drag ratio can be determined.

DATA AND RESULTS

After careful and extensive calibration of the sting and water tunnel, the following lift and drag values as a function of angle of attack were obtained for each of the four wing configurations.

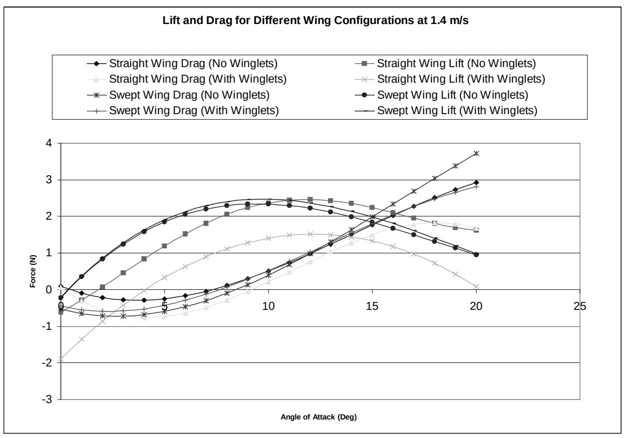

Fig. 7. Lift and Drag for Different Wing Configurations at 1.4 m/s

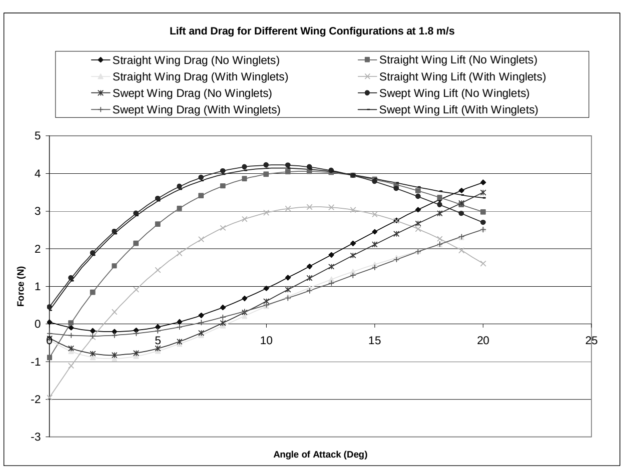

Fig. 8. Lift and Drag for Different Wing Configurations at 1.8 m/s

These values are then converted to lift to drag ratios and are shown below.

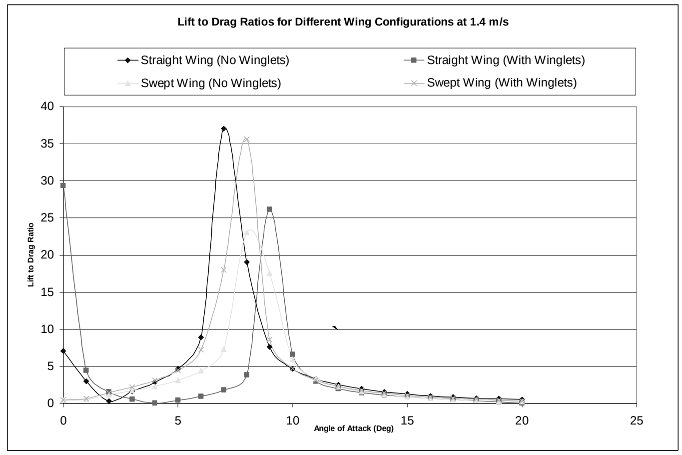

Fig. 9. Lift to Drag Ratios for Different Wing Configurations at 1.4 m/s

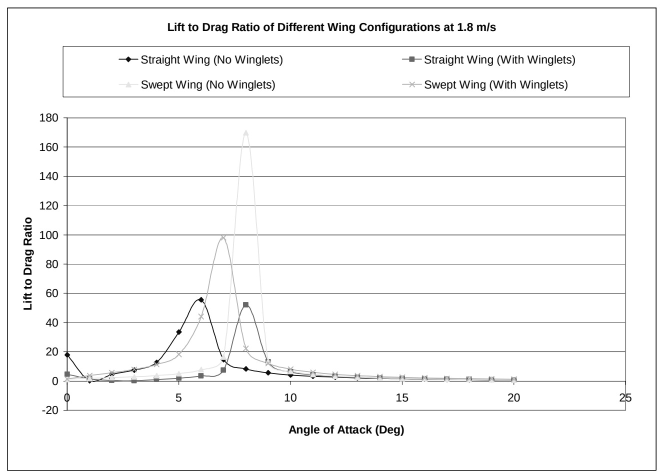

Fig. 10. Lift to Drag Ratio of Different Wing Configurations at 1.8 m/s

DISCUSSION AND CONCLUSIONS

As is theoretically expected, the lift to drag ratio of any wing is a function of angle of attack. The experimental analysis for all wing configurations with the NACA 0012 symmetric foil showed that a maximum lift to drag ratio was obtained at angles of attack between six and nine degrees. A maximum lift to drag ratio of 37 and 23 for the straight and swept back wings with no winglets, respectively, was obtained at a velocity of 1.4 m/s. To verify these experimental values, lift to drag ratios were also determined at a velocity of 1.8 m/s. A maximum lift to drag ratio of about 56 and 170 for the straight and swept back wings with no winglets, respectively, was obtained. This is an increase in lift to drag ratio of about 50% for the straight wing and 638% for the swept back wing. Although the swept back wing without winglets showed the maximum lift to drag ratio of 170, it is clear from relative values of the other wing configurations and empirical data, that this ratio is abnormally high and can be disregarded. In theory, the lift to drag ratio should not have a major dependence on velocity, but primarily be dependent on the angle of attack. Our experimental data clearly doesn't demonstrate that, since the experimental values showed that as the speed increased the lift to drag ratio of all wing configurations increase. This is most likely due to sting calibration. A closer look of all the lift and drag curves for all wing configurations reveals a negative drag for small angles of attack. This is a clear contradiction to the laws of physics, since a negative drag is not possible in this configuration. It can also be noted that on the straight wing configurations, at zero angle of attack, the wing produces a slight negative lift, which is apparent since zero lift is achieved at an angle of attack of about three degrees. This is most likely caused by the wing's chord line not being perfectly parallel to the axial beam when mounted.

The effect of winglets on the lift to drag ratio on both wing configurations was also studied. Winglets decreased the ratio for the straight wing at both velocities. At low velocity, the straight wing without winglets had a higher ratio compared to that of the swept wing with winglets. It was determined that at a velocity of 1.4 m/s, the addition of winglets decreases the lift to drag ratio of the straight wing by about 30%, but the lift to drag ratio of the swept back wing increased to 36, an increase of 55%. Whereas at a speed of 1.4 m/s the addition of winglets increased the lift to drag ratio of a swept back wing, the opposite effect resulted on both the straight and swept back wing at a higher velocity. At 1.8 m/s, the lift to drag ratio of the straight wing decreased from 56 to 52, a decrease of about 6%. However, the addition of winglets on the swept back wing was a little more dramatic. The lift to drag ratio decreased from 170 to 98, a decrease of about 42%. This value will be disregarded due to the correlating values of the other wing configurations and from values determined at the lower velocity.

A summary of all the combined data taken for the different wing configurations and disregarding the abnormally high ratio of the swept wing with no winglets, shows that winglets decreased the lift to drag ratio for the straight wing, but increased the ratio for the swept wing. Due to the consistency of the lift to drag ratio of the swept wing with winglets for both velocities, it is determined this configuration provides the highest lift to drag ratio of 97.9 ± 0.2. Although data taken at only 2 different water velocities is not completely conclusive, due to the consistency of the lift to drag ratio of the swept wing with winglets for both velocities, it was determined that a swept back wing with winglets is the configuration that provides the highest lift to drag ratio at an angle of about 7 degrees. Thus, implementation of a tail with a swept back wing with winglets will best propel the UCSD Human Powered Submarine to a very achievable IHPVA and World Record.

ERROR ANALYSIS

I. a. Sample Calibration of Angle of Attacks

An error of 0.3 degrees is estimated for the calculated angle of attack. Using the calibration curve, the number of turns was found to be:

$$N = 1.0123*A + 9.2838 = 9.3 \text{ turns} \qquad (24)$$

$$\delta N = 1.0123\delta A = 0.3 \text{ turns} \qquad (25)$$

where N is the number of turns and A is the angle of attack.

I. b. Sample Calibration of Normal and Axial Forces

With a 0.219kg mass hung from the sting in the horizontal position, an average voltage was obtained for the normal force at zero angle of attack:

$$V_{ave} = \sum x_i/N = -2.112V \quad (26)$$

where $\sum x$ is the sum of the voltages and N is the number of data points collected. The error of this equation, or the standard deviation, is:

$$\delta V = \sigma_V = ((1/(N-1))\sum(x_i - x_{ave})^2)^{1/2} = 0.005V \quad (27)$$

The voltages were correlated to weight values by making a calibration curve of voltage vs. force. But first, the mass values were converted into weight values by multiplying by gravity. For a mass of 0.219 kg, the weight and the error on this value was determined assuming that the mass had an error of 0.001 kg:

$$W = mg = 2.148N \quad (28)$$

$$\delta W = \delta m * g = 0.002N \quad (29)$$

I. c. Sample Calibration of Water Tunnel Using the Pitot-Static Tube

Inches of water from the Pitot-Static tube is obtained by equation 20:

$$\Delta h = 1.6325V + 0.0068 = 1.6325*0.44 + 0.0068 = 0.73in$$

after converting to meters $\Delta h \approx 0.0184m$. An error of this equation is obtained as follows:

$$\delta h = (dy/dx)* \delta V= (1.6325)*(.01) \approx 0.0004 \text{ m} \quad (30)$$

where dy/dx is equal to the slope of Δh, and δV is the error in the voltage reading, which we assumed to be approximately equal to 0.01. The mean velocity reading is obtained by equation 21:

$$U_\infty = (2\Delta hg)^{1/2} = [(0.018216*9.81)]^{1/2} \approx 0.601 \text{ m/s}$$

An error of this equation is obtained as follows:

$$\delta U=U[0.5*\delta h/h]=0.6[0.5*0.2/0.018216]\approx 0.007 \text{ m/s} \quad (31)$$

I. d. Sample Calibration of Water Force on Sting

At a velocity of 0.6 m/s, an average voltage was obtained for the normal force at zero angle of attack using equation 26:

$$V_{ave}=\sum x_i/N=-0.008V$$

where $\sum x$ is the sum of the voltages and N is the number of data points collected. The error of this equation, or the standard deviation, was found with equation 27:

$$\delta V=\sigma_V=((1/(N-1))\sum(x_I-x_{ave})^2)^{1/2}= 0.024V$$

II.a. Sample Wing Test

At a velocity of 1.4 m/s, the normal voltage and error at zero angle of attack was found again using equations 26 and 27:

$$V_{ave} = \sum x_i/N = 1.019V$$

$$\delta V = \sigma_V = ((1/(N-1))\sum(x_I-x_{ave})^2)^{1/2} = 0.007V$$

II.b. Sample Drag Calculation

The drag for the swept wing with winglets at 1.4 m/s was found using equation 18:

$$Drag = [0.7489(\text{axialvoltage})+0.1196+0.00006(\alpha)^4-.0025(\alpha)^3+0.0429(\alpha)^2-0.2413(\alpha)-0.047((-1.0257(\text{normal voltage})+0.0021)/\cos(\alpha)+0.0086(\alpha)+0.3411(V_w)^2-0.2247(V_w))+0.002(\alpha)^2-0.0094(\alpha)+0.0012(\alpha)^2+0.0342(\alpha)-0.1692(V_w)-0.3863(V_w)]/(1-0.047*\sin(\alpha)/\cos(\alpha))=0.07N$$

$$\delta F_D = F_D \sqrt{\left(\frac{\sqrt{\delta A^2 + \delta B^2 + \delta C^2}}{D}\right)^2 + \left(\sqrt{\left(\frac{0.047\,\delta\alpha\cos\alpha}{0.047\sin\alpha}\right)^2 + \left(\frac{\delta\alpha\sin\alpha}{\cos\alpha}\right)^2}\right)^2}$$

where

$$\delta A = \sqrt{\left(0.7489\,\delta_{axialvolts}\right)^2 + \left(4\alpha^3\delta\alpha(6E-5)\right)^2 + \left(3\alpha^2\delta\alpha(0.0025)\right)^2 + \left(2\alpha\delta\alpha(0.0429)\right)^2}$$

$$\delta B = (0.047)\sqrt{\left(\left(\frac{(1.0257)(normalvolts)}{\cos\alpha}\right)\sqrt{\left(\frac{\delta_{normalvolts}}{normalvolts}\right)^2 + \left(\frac{\delta\alpha\sin\alpha}{\cos\alpha}\right)^2}\right)^2 + (0.0086\,\delta\alpha)^2 + \left(2V_W\delta V_W(0.3411)\right)^2 + \left(0.2247\,\delta V_W\right)^2}$$

$$\delta C = \sqrt{\left(2\alpha\delta\alpha(0.002)\right)^2 + (0.0094\,\delta\alpha)^2 + \left(2\alpha\delta\alpha(0.0012)\right)^2 + (0.0342\,\delta\alpha)^2 + \left(2V_W\delta V_W(0.1692)\right)^2 + \left(0.3863\,\delta V_W\right)^2}$$

$$D = (0.7489)(axialvolts) + 0.1196 + (6E-5)\alpha - 0.0025\alpha^3 + 0.0429\alpha^2 - 0.2413\alpha - (0.047)\left[\frac{(-1.0257)(normalvolts) + 0.0021}{\cos\alpha} + 0.0086\alpha + 0.3411V_W^{\,2} - 0.2247V_W\right] + 0.002\alpha^2 - 0.0094\alpha + 0.0012\alpha^2 + 0.0342\alpha - 0.1692V_W^{\,2} - 0.3863V_W$$

$$\delta F_D = 0.03\text{N} \qquad (32)$$

II.c. Sample Lift Calculation

For a straight wing with no winglets, lift was calculated using equation 19:

$$\text{Lift} = [-1.0257(\text{normalvoltage}) + 0.0021 - \text{Drag}*\sin(\alpha)]/\cos(\alpha) + 0.0086(\alpha) + 0.3411(V_w) - 0.2247(V_w) = 2.3987\text{N}$$

$$\delta F_L = \left[\left[\left|\frac{(-1.0257)(normalvolts) + 0.0021 - F_D\sin\alpha}{\cos\alpha}\right| \text{X} \left[\left(\frac{\sqrt{(|-1.0257|\delta_{normalvolts})^2 + \left(|F_D\sin\alpha|\sqrt{\left(\frac{\delta F_D}{F_D}\right)^2 + \left(\frac{|\cos\alpha|\delta\alpha}{\sin\alpha}\right)^2}\right)^2}}{(-1.0257)(normalvolts) + 0.0021 - F_D\sin\alpha}\right)^2 + \left(\frac{|-\sin\alpha|\delta\alpha}{\cos\alpha}\right)^2\right]^{1/2}\right]^2 + \left[|-0.0086|\delta\alpha\right]^2 + \left[\frac{2|-0.3411||V_W^{\,2}|\delta V_W}{|V_W|}\right]^2 + \left[|0.2247|\delta V_W\right]^2\right]$$

$$\delta F_L = 0.03\text{N} \qquad (33)$$

II.d. Sample Calculation of Lift to Drag Ratio

The lift to drag ratio of a straight wing with no winglets was found using:

$$\text{Ratio} = \text{Lift/Drag} = 35.6 \qquad (34)$$

$$\delta L/D = ((\delta D/D)^2 + (\delta L/L)^2)^{1/2} = 0.3 \qquad (35)$$

REFERANCES

1. Introduction to Fluid Mechanics, Fox & McDonald, John Wiley & Sons Inc., 5th Ed

2. An Introduction to Error Analysis, John R. Taylor, University Science Books, 1982

3. The Emergence of Whales, "Biomechanical Perspective of the Origin of Cetacean Flukes", Frank E. Fish, Plenum Press, 1998

APPENDIX

Sting Design and Analysis

The maximum lift and drag forces on the NACA 0012 foil from equations 1 and 2 are:

$$L = 0.5\rho V^2 C_L A_p = 0.5(1000\text{kg/m}^3)(3\text{m/s})^2(1.2)(0.0039\text{m}^2) = 20.9\text{N}$$

$$D = 0.5\rho V^2 C_D A_p = 0.5(1000\text{kg/m}^3)(3\text{m/s})^2(0.8)(0.0039\text{m}^2) = 13.9\text{N}$$

The moment of inertia of cantilevered axial beam, made of Aluminum 6061-T6, was calculated with L=6.5 inches (0.2286m) and θ_{max}=1 degree=0.0175 radians using equation 4:

$$I = PL^2/2E\theta$$
$$= (20.9\text{N})(0.1651\text{m})^2/(2)(70\text{x}10^9)(0.0175\text{rad}) = 2.33\text{x}10^{-10}\text{ m}^4$$

From this, the height, h, of the axial beam was calculated with width, b, defined as 3/16in or 0.00476m using equation 3:

$$h = (12I/b)^{1/3} = ((12)(2.33\text{x}10^{-10}\text{m})/(0.00476\text{m}))^{1/3} = 0.00837\text{m} = 0.330\text{in}$$

A more standard dimension for h would be 3/8in or 0.00953m. The moment of inertia, slope, and deflection for these final dimensions are from equations 3, 4, and 5 are:

$I=1/12bh^3 = (1/12)(0.0047m6)(0.00953m)^3=3.43 \times 10^{-10} m^4$

$\theta=PL^2/2EI=(20.9N)(0.1651m)^2/(2)(70x10^9Pa)(3.43x10^{-10} m^4)= 0.68$ deg

$\delta=PL^3/3EI=(20.9N)(0.1651m)^3/(3)(70x10^9Pa)(3.43x10^{-10} m^4) = 0.0492$ in

The stress and strain for this beam at 5.5in from the end are calculated with equations 6 and 7:

$\sigma_{xy}=Pxy/I=(20.9N)(0.1397m)(0.00476m)/(3.43x10^{-10} m^4)=38798767Pa$

$\varepsilon = \sigma_{xy}/E = (38798767Pa)/(70x10^9Pa)= 0.0005543$

Finally, the stress and strain for the normal beam at 3 inches from the end are determined using the same procedure with b=3/16in or 0.0047m and h=1/4in or 0.00635m using equations 3, 6, and 7:

$I=1/12bh^3 = (1/12)(0.0047m6)(0.00635m)^3=1.016x10^{-10} m^4$

$\sigma_{xy}=Pxy/I=(13.9N)(0.0762m)(0.003175m)/(1.016x10^{-10}m^4)= 33099375Pa$

$\varepsilon=\sigma_{xy}/E=(33099375Pa)/(70x10^9Pa)= 0.000473$